Mid-infrared integrated photonics on silicon: a perspective

Qiankun Liu, Joan Manel Ramirez, Vladyslav Vakarin, Xavier Le Roux, Andrea Ballabio, Jacopo Frigerio, Daniel Chrastina, Giovanni Isella, David Bouville, Laurent Vivien, et al.

Research Article | Vol. 8, No. 5 | 1 May 2018 | OPTICAL MATERIALS EXPRESS 1305
Optical Materials EXPRESS

Mid-infrared sensing between 5.2 and 6.6 μm wavelengths using Ge-rich SiGe waveguides [Invited]

Qiankun Liu,[1] Joan Manel Ramirez,[1] Vladyslav Vakarin,[1] Xavier Le Roux,[1] Andrea Ballabio,[2] Jacopo Frigerio,[2] Daniel Chrastina,[2] Giovanni Isella,[2] David Bouville,[1] Laurent Vivien,[1] Carlos Alonso Ramos,[1] and Delphine Marris-Morini[1,*]

[1]*Centre de Nanosciences et de Nanotechnologies, Université Paris Sud, CNRS, Université Paris Saclay, 91405 Orsay, France*
[2]*L-NESS, Dipartimento di Fisica, Politecnico di Milano, Polo di Como, Via Anzani 42, 22100 Como, Italy*
**delphine.morini@u-psud.fr*

Abstract: Mid-infrared (mid-IR) integrated photonics are expected to provide key advances for the demonstration of chip-scale spectroscopic systems. It has been recently reported that Ge-rich SiGe alloy-based photonic structures can provide broadband operation for a wavelength range spanning from 5.5 to 8.5 μm, thus holding great potential for mid-IR applications. In this paper, the Ge-rich SiGe platform is considered for a mid-IR photonic chip-scale sensor, based on the use of the evanescent component of the guided optical mode to probe specific molecular absorption features of the surrounding cladding environment. As a proof of concept, we monitored the absorption spectral patterns of a standalone photoresist spin-coated onto spiral Ge-rich SiGe waveguides. A significant increase of the waveguide optical loss at the spectral window of 5.8-6.2 μm is identified and correlated with the inherent photoresist absorption. The ability of this platform to sense small concentrations of methane gas is also discussed. These results pave the way towards the demonstration of compact, portable, label-free and highly sensitive photonic integrated sensors based on Ge-rich SiGe circuits.

OCIS codes: (130.0130) Integrated optics; (130.6010) Sensors; (300.6340) Spectroscopy, infrared.

References and links

1. H. Lin, Y. Song, Y. Huang, D. Kita, S. Deckoff-Jones, K. Wang, L. Li, J. Li, H. Zheng, Z. Luo, H. Wang, S. Novak, A. Yadav, C.-C. Huang, R.-J. Hiue, D. Englund, T. Gu, D. Hewak, K. Richardson, J. Kong, and J. Hu, "Chalcogenide glass-on-graphene photonics," Nat. Photonics **11**(12), 798–805 (2017).
2. M. Muneeb, A. Ruocco, A. Malik, S. Pathak, E. Ryckeboer, D. Sanchez, L. Cerutti, J. B. Rodriguez, E. Tournié, W. Bogaerts, M. K. Smit, and G. Roelkens, "Silicon-on-insulator shortwave infrared wavelength meter with integrated photodiodes for on-chip laser monitoring," Opt. Express **22**(22), 27300–27308 (2014).
3. H. Lin, Z. Luo, T. Gu, L.-C. Kimerling, K. Wada, A. Agarwal, and J. Hu, "Mid-infrared integrated photonics on silicon: a perspective," Nanophotonics **7**(2), 85 (2017).
4. A.-Z. Subramanian, E. Ryckeboer, A. Dhakal, F. Peyskens, A. Malik, B. Kuyken, H. Zhao, S. Pathak, A. Ruocco, A. De Groote, P. Wuytens, D. Martens, F. Leo, W. Xie, U. Dave, M. Muneeb, P. Van Dorpe, J. Van Campenhout, W. Bogaerts, P. Bienstman, N. Le Thomas, D. Van Thourhout, Z. Hens, G. Roelkens, and R. Baets, "Silicon and silicon nitride photonic circuits for spectroscopic sensing on-a-chip," Photon. Res. **3**(5), 47–59 (2015).
5. M. Nedeljkovic, J. S. Penades, V. Mittal, G. S. Murugan, A.-Z. Khokhar, C. Littlejohns, L.-G. Carpenter, C. B. E. Gawith, J.-S. Wilkinson, and G.-Z. Mashanovich, "Germanium-on-silicon waveguides operating at mid-infrared wavelengths up to 8.5 μm," Opt. Express **25**(22), 27431–27441 (2017).
6. A. Gutierrez-Arroyo, E. Baudet, L. Bodiou, J. Lemaitre, I. Hardy, F. Faijan, B. Bureau, V. Nazabal, and J. Charrier, "Optical characterization at 7.7 μm of an integrated platform based on chalcogenide waveguides for sensing applications in the mid-infrared," Opt. Express **24**(20), 23109–23117 (2016).
7. Z. Han, P. Lin, V. Singh, L. Kimerling, J. Hu, K. Richardson, A. Agarwal, and D. T. H. Tan, "On-chip mid-infrared gas detection using chalcogenide glass waveguide," Appl. Phys. Lett. **108**(14), 141106 (2016).

#322985 https://doi.org/10.1364/OME.8.001305
Journal © 2018 Received 12 Feb 2018; revised 12 Apr 2018; accepted 12 Apr 2018; published 24 Apr 2018

Optical Materials EXPRESS

8. Y. Chen, H. Lin, J. Hu, and M. Li, "Heterogeneously integrated silicon photonics for the mid-infrared and spectroscopic sensing," ACS Nano **8**(7), 6955–6961 (2014).
9. Y.-C. Chang, P. Wägli, V. Paeder, A. Homsy, L. Hvozdara, P. van der Wal, J. Di Francesco, N. F. de Rooij, and H. Peter Herzig, "Cocaine detection by a mid-infrared waveguide integrated with a microfluidic chip," Lab Chip **12**(17), 3020–3023 (2012).
10. B. Schwarz, P. Reininger, D. Ristanić, H. Detz, A. M. Andrews, W. Schrenk, and G. Strasser, "Monolithically integrated mid-infrared lab-on-a-chip using plasmonics and quantum cascade structures," Nat. Commun. **5**, 4085 (2014).
11. S.-A. Miller, M. Yu, X. Ji, G. Griffith, J. Cardenas, A.-L. Gaeta, and M. Lipson, "Low-loss silicon platform for broadband mid-infrared photonics," Optica **4**(7), 707–712 (2017).
12. P.-T. Lin, V. Singh, J. Hu, K. Richardson, J.-D. Musgraves, I. Luzinov, J. Hensley, L.-C. Kimerling, and A. Agarwal, "Chip-scale Mid-Infrared chemical sensors using air-clad pedestal silicon waveguides," Lab Chip **13**(11), 2161–2166 (2013).
13. M. Nedeljkovic, A. Z. Khokhar, Y. Hu, X. Chen, J. Soler Penades, and S. Stankovic, "Silicon photonic devices and platforms for the mid-infrared," Opt. Mater. Express **3**(9), 1205–1214 (2013).
14. J. Soler Penadés, C. Alonso-Ramos, A. Z. Khokhar, M. Nedeljkovic, L. A. Boodhoo, A. Ortega-Moñux, I. Molina-Fernández, P. Cheben, and G. Z. Mashanovich, "Suspended SOI waveguide with sub-wavelength grating cladding for mid-infrared," Opt. Lett. **39**(19), 5661–5664 (2014).
15. R. Soref, "Mid-infrared photonics in silicon and germanium," Nat. Photonics **4**(8), 495–497 (2010).
16. Y.-C. Chang, V. Paeder, L. Hvozdara, J.-M. Hartmann, and H.-P. Herzig, "Low-loss germanium strip waveguides on silicon for the mid-infrared," Opt. Lett. **37**(14), 2883–2885 (2012).
17. S. Kim, J.-H. Han, J.-P. Shim, H.-J. Kim, and W.-J. Choi, "Verification of Ge-on-insulator structure for a mid-infrared photonics platform," Opt. Mater. Express **8**(2), 440–451 (2018).
18. L. Carletti, M. Sinobad, P. Ma, Y. Yu, D. Allioux, R. Orobtchouk, M. Brun, S. Ortiz, P. Labeye, J. M. Hartmann, S. Nicoletti, S. Madden, B. Luther-Davies, D. J. Moss, C. Monat, and C. Grillet, "Mid-infrared nonlinear optical response of Si-Ge waveguides with ultra-short optical pulses," Opt. Express **23**(25), 32202–32214 (2015).
19. M. Brun, P. Labeye, G. Grand, J.-M. Hartmann, F. Boulila, M. Carras, and S. Nicoletti, "Low loss SiGe graded index waveguides for mid-IR applications," Opt. Express **22**(1), 508–518 (2014).
20. J.-M. Ramirez, Q. Liu, V. Vakarin, J. Frigerio, A. Ballabio, X. Le Roux, D. Bouville, L. Vivien, G. Isella, and D. Marris-Morini, "Graded SiGe waveguides with broadband low-loss propagation in the mid infrared," Opt. Express **26**(2), 870–877 (2018).
21. V. Vakarin, J.-M. Ramírez, J. Frigerio, A. Ballabio, X. Le Roux, Q. Liu, D. Bouville, L. Vivien, G. Isella, and D. Marris-Morini, "Ultra-wideband Ge-rich silicon germanium integrated Mach-Zehnder interferometer for mid-infrared spectroscopy," Opt. Lett. **42**(17), 3482–3485 (2017).
22. N.-K. Hon, R. Soref, and B. Jalali, "The third-order nonlinear optical coefficients of Si, Ge, and Si1- xGex in the midwave and longwave infrared," J. Appl. Phys. **110**(1), 011301 (2011).
23. S. Serna, V. Vakarin, J.-M. Ramirez, J. Frigerio, A. Ballabio, X. Le Roux, L. Vivien, G. Isella, E. Cassan, N. Dubreuil, and D. Marris-Morini, "Nonlinear Properties of Ge-rich $Si_{1-x}Ge_x$ Materials with Different Ge Concentrations," Sci. Rep. **7**(1), 14692 (2017).
24. J. M. Ramirez, V. Vakarin, J. Frigerio, P. Chaisakul, D. Chrastina, X. Le Roux, A. Ballabio, L. Vivien, G. Isella, and D. Marris-Morini, "Ge-rich graded-index Si1-xGex waveguides with broadband tight mode confinement and flat anomalous dispersion for nonlinear mid-infrared photonics," Opt. Express **25**(6), 6561–6567 (2017).
25. http://cmnst.ncku.edu.tw/ezfiles/23/1023/img/127/s1800seriesDataSheet.pdf
26. B. Tuzson, J. Jágerská, H. Looser, M. Graf, F. Felder, M. Fill, L. Tappy, and L. Emmenegger, "Highly Selective Volatile Organic Compounds Breath Analysis Using a Broadly-Tunable Vertical-External-Cavity Surface-Emitting Laser," Anal. Chem. **89**(12), 6377–6383 (2017).
27. L. Tombez, E. J. Zhang, J. S. Orcutt, S. Kamlapurkar, and W. M. J. Green, "Methane absorption spectroscopy on a silicon photonic chip," Optica **4**(11), 1322–1325 (2017).
28. International Chemical Safety Cards (ICSC) of the National Institute for Occupational Safety and Health, (NIOSH), "Methane ICSC # 0291. CAS #: 74-82-8 (2010)", http://www.cdc.gov/niosh/ipcsneng/neng0291.html

1. Introduction

In the recent years, key advances towards the development of on-chip photonic platforms exploiting the mid-Infrared (mid-IR) wavelength range have been made [1–5]. On-chip sensing systems able to trace specific mid-IR molecular absorption patterns efficiently are nowadays driving most of the efforts, providing new routes towards the implementation of novel sensor technologies with several killer applications such as real-time accurate monitoring of greenhouse gases. So far, most of the proposed integrated sensors rely on the monitoring of the absorption perturbations of the evanescent propagating waves of guided optical modes [6–9], although other sensing mechanisms have also been proposed based on surface plasmon polariton waveguides [10].

Optical Materials EXPRESS

Besides photonic platforms as chalcogenide glasses or III-V materials, silicon (Si) photonics is also meant to have high impact in the mid-IR technology. Indeed, silicon photonics solutions have already been successfully implemented at near-IR wavelengths, providing a reliable and high volume platform that leverages from a standalone and mature technology that has been largely employed by now to develop microelectronic integrated circuits [3]. However, the extension of the operation wavelength range of conventional silicon-on-insulator (SOI) waveguides towards the mid-IR is limited by the buried SiO_2 layer, which shows a strong and continuous optical absorption for wavelengths beyond $\lambda = 3.6$ μm. In order to circumvent this situation, alternative approaches to extend the operating wavelength of Si-based photonics integrated circuits towards the mid-IR have been proposed, including the implementation of waveguide engineering strategies to minimize the mode overlap with the surrounding cladding [11], the use of pedestal under-cladding geometry [12] or the development of suspended membranes [13,14]. In any case, the use of silicon as a waveguide core limits the largest available wavelength for low-loss operation at values below 8 μm, in accordance with the Si mid-IR transparency window. This fact prevents Si photonic platforms from accessing to an important family of biological and chemical substances that present absorption patterns within the $\lambda = 8$-13 μm spectral window. Then, alternatives able to exploit larger wavelengths in an efficient manner have to be developed. Among the materials compatible with large-scale silicon photonic integration, Germanium (Ge) is particularly compelling. Indeed, Ge has the largest transparency window in the group IV materials, from 1.5 to 14.7 μm [15]. Different solutions have thus been explored including Ge on Si [5, 16], Ge on insulator (GeOI) [17], SiGe on Si [18], or graded SiGe/Si waveguides [19].

Ge-rich SiGe waveguides have been recently identified as a promising solution to take benefit from such large transparency window of Ge. Wideband operation of spiral waveguides and Mach Zehnder interferometers from 5.5 to 8.5μm has been recently reported [20, 21]. Interestingly, a strong increase of the third-order nonlinear optical properties with the Ge concentration larger than 80% was theoretically predicted [22] and confirmed experimentally [23], demonstrating the huge potential of such platform for active devices based on non-linear effects such as a broadband supercontinuum sources [24].

In this paper we report the first proof of concept of an integrated mid-IR evanescent sensor based on Ge-rich SiGe waveguides. For the purpose of this demonstration, we recorded the specific mid-IR absorption feature of a photoresist spin-coated onto the waveguides. Finally, sensing capabilities of methane gas based on such Ge-rich SiGe platform are discussed.

2. Methods and materials

In this study, a $Si_{0.2}Ge_{0.8}$ waveguide on graded $Si_{1-x}Ge_x$ is considered as the building block of the mid-IR photonic circuit. Low-energy plasma-enhanced chemical vapor deposition was used for the material growth on Si substrate. The Ge concentration was increased linearly from 0 to 0.79 along the growth direction over 11 μm thickness with a growth rate of 5–10 nm/s. Then a 2 μm thick $Si_{0.2}Ge_{0.8}$ guiding layer was grown on top of the graded layer. The structures were patterned using optical lithography, followed by inductively coupled plasma etching. The etching depth was 4 μm and the waveguide width was 5 μm, as illustrated in Fig. 1(a); the fundamental TE mode profile is reported in Fig. 1(b). The low dispersion of this waveguide is illustrated by the mode calculation reported in Fig. 1(c) from where it can be seen that the effective index variations of the fundamental TE and TM modes are lower than 0.1 for wavelengths varying from 5.5 to 8.5 μm. Spiral waveguides (see Fig. 1(e)) have thus been defined with lengths of 0.6 cm; 4.2 cm; 6.1 cm; and 8.3 cm, allowing precise measurement of propagation loss using a non-destructive cut-back method. A minimum bend radius of 600 μm was set for the spiral to preclude unwanted radiative loss and mode coupling in the bending. During the experiments, the optical mode profile of the waveguide output is inspected using a mid-IR camera. Only fundamental modes are obtained at the

Optical Materials EXPRESS

waveguide output, indicating a proper optical coupling in the fundamental TE or TM modes and negligible mode coupling to higher order modes within the photonic circuit. The transmission properties of similar spirals, but without any cladding have been previously studied in [20]. Flat transmission was reported between 5.5 and 8.5 µm wavelength for both TE and TM polarizations, with propagation losses between 2 and 3 dB/cm in the full wavelength range.

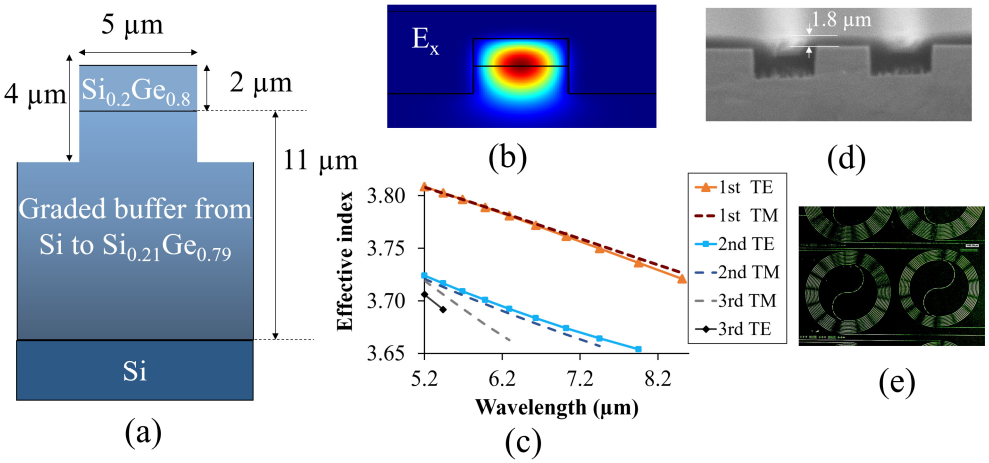

Fig. 1. (a) schematic cross-section of the waveguide under consideration: a 11µm-thick graded SiGe layer from Si to $Si_{0.21}Ge_{0.79}$ is followed by a 2 µm-thick $Si_{0.2}Ge_{0.8}$ layer. The waveguide width is 5 µm and the etching depth is 4 µm (b) Simulated fundamental TE mode at λ = 6 µm (c) dispersion curve of the waveguide covered by photoresist (d) SEM view of the waveguide covered by the S1818 photoresist (e)Top view of the fabricated sample

The sensing capability of the Ge-rich SiGe platform has been assessed using a convenient and easy-to-manipulate approach. For that, we covered the waveguide with S1818 photoresist [25] (thickness of ~1.8 µm) and studied the transmission spectrum for different waveguide lengths. The SEM view of the waveguide (Fig. 1(d)) confirms that the photoresist fully covers the top surface and the side facets of the waveguide. The evanescent component of the guided mode thus interacts with the photoresist cladding, resulting in wavelength-specific transmission absorption bands. Hence, the comparison of waveguide transmission with and without photoresist allows us to demonstrate the sensing concept in Ge-rich SiGe waveguides.

Finally, in order to corroborate the results, the photoresist transmission properties have been characterized in a non-guided-based experimental configuration. 78-µm-thick photoresist has been deposited on top of a Si sample by a repetition of 15 steps of spin-coating/annealing process, and transmission has been measured by illuminating the sample from top surface. The mid-IR experimental set-up used for both experiments was described previously in Ref [20].

3. Results and discussion

3.1 Characterization of the photoresist

First, the mid-IR transmission characteristics of the photoresist have been measured using the surface illumination configuration. For this purpose, the transmission of a Si sample covered by 78-µm-thick photoresist was normalized by the transmission of a Si wafer (without photoresist). The absorption coefficient of the photoresist was then deduced, being the result reported in Fig. 2. For the sake of comparison, the absorption coefficient of the Si wafer has been measured separately and is reported in the same figure. It can be seen that the

Optical Materials EXPRESS

photoresist exhibits a clear wavelength-dependent transmission spectrum, showing strong absorption features at 5.86 µm and at 6.25 µm wavelengths. These peaks correspond to absorption coefficients of 950 and 613 cm^{-1}, respectively. Absorption coefficients in excess of 1000 cm^{-1} appear at different wavelengths beyond 6.6 µm.

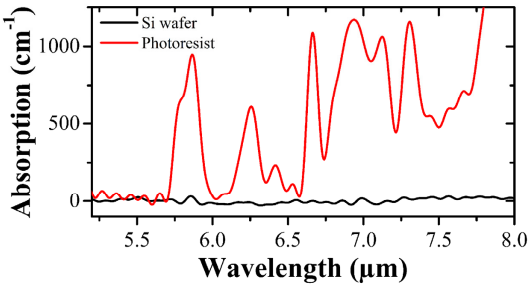

Fig. 2. Absorption coefficient of the photoresist. Strong absorption peaks can be seen at 5.86 µm and 6.25 µm. Absorption coefficient larger than 1000 cm^{-1} is even obtained for wavelengths larger than 6.6 µm.

3.2 Transmission measurements of the Ge-rich SiGe spiral waveguides with photoresist cladding

The transmission spectra of the Ge-rich SiGe spiral waveguides with and without the cladding have been measured for both TE and TM polarizations. The measurements, which have been normalized by the set-up transmission, are reported in Fig. 3 for TE-polarized optical signals. Interestingly, the absorption peaks of the photoresist at 5.86 µm and 6.25 µm wavelengths are clearly observed in the transmitted spectra of the sample with cladding (Fig. 3.(b)), being deeper for longer spiral lengths. These absorption features are not seen in the measurement without cladding (Fig. 3(a)). These results prove the ability of Ge-rich SiGe waveguide to probe mid-IR absorption features through evanescent-field-mediated light-matter interactions.

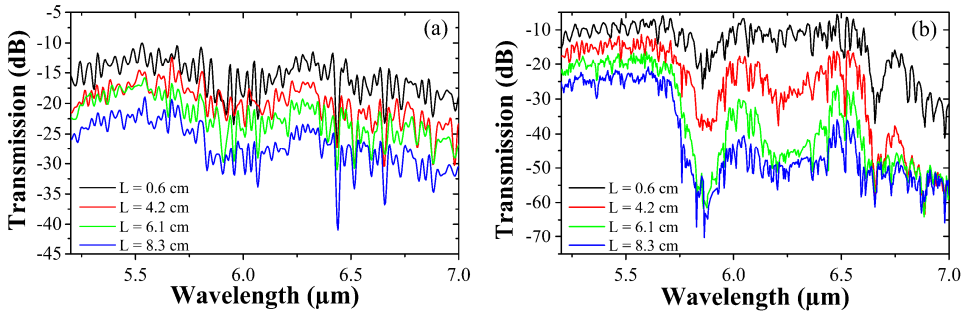

Fig. 3. Raw transmission measurement of the spiral waveguides of different lengths (normalized by the set-up transmission with no sample) (a) without and (b) with photoresist cladding, for a TE-polarized optical mode. Interestingly the absorption features of the photoresist at 5.86 µm and 6.25 µm wavelength can be clearly seen in the transmitted spectra of the spin-coated sample. For wavelengths larger than 6.6 µm, the transmission of the waveguides covered by the photoresist is too low to be correctly measured, therefore being limited by the strong photoresist absorption used as waveguide cladding. The minimum detectable transmission of the experimental set-up (noise level) is around –65 dB.

The set of spiral waveguides with lengths from 0.6 to 8.3 cm can be used to deduce propagation loss of the waveguides by a non-destructive cut-back method with a precision better than ± 0.5dB/cm. As an example, the transmittance at 5.6 µm wavelength is reported in the inset of Fig. 4, showing a linear decrease with the spiral length whose slope can be used to deduce the guided mode optical loss. The deduced optical loss spectrum is reported in Fig.

Optical Materials EXPRESS

4(a) for both TE and TM modes, obtaining a similar performance. For wavelengths lower than 5.7 µm, a propagation loss of 2 dB/cm is obtained, which is in line with previously reported results on the same platform [20]. Optical losses then increase to reach 7 dB/cm at 5.86 µm and 6.2 dB/cm at about λ = 6.25 µm. For wavelengths larger than 6.6 µm, the transmission of the waveguides covered by the photoresist is too low to be correctly measured, which is compatible with the high value (> 1000 cm^{-1}) of the absorption coefficient of the photoresist used as waveguide cladding at these wavelengths (see Fig. 2).

The comparison of the waveguide loss and the photoresist's absorption coefficient at 6.25 µm wavelength allows us to estimate the overlap factor of the optical mode with the absorbing cladding, being 0.16% for the TE mode and 0.17% for the TM mode propagation. Noticeably, these values are a bit lower than the theoretical value obtained from mode simulations (0.29% and 0.30%, respectively). The slight difference between calculations and experiments could be attributed to an over-estimation of the photoresist's absorption coefficient in the surface illumination experiment, which may result in an effective reduction of the estimated overlap factor. However, in order to be conservative, we consider an overlap value of 0.17% in the following discussion. This is indeed a pessimistic value to evaluate the sensing capabilities of the Ge-rich SiGe waveguides. However, it is worth noting that besides the exact value of the overlap factor, the comparison of the general shape of the waveguide propagation loss and the photoresist's absorption coefficient reported in Fig. 4(b) shows an excellent correlation between both measurements, demonstrating the outstanding sensing properties of the Ge-rich SiGe spiral waveguides.

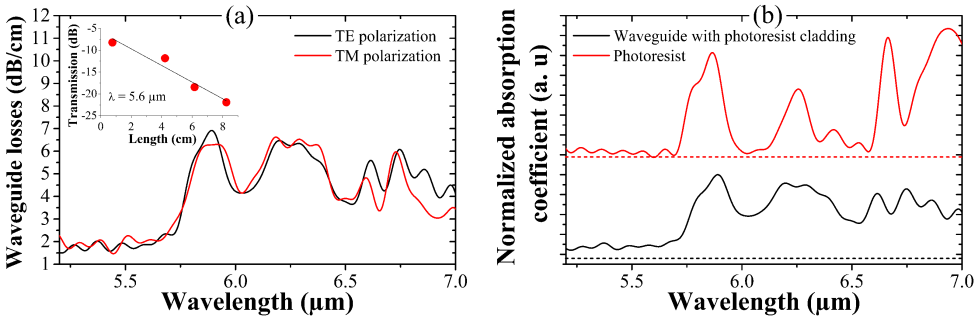

Fig. 4. (a) Propagation loss of the Ge-rich SiGe waveguide covered by photoresist, for TE-and TM-polarized optical modes. The photoresist's absorption features at 5.86 µm and 6.25 µm wavelength can be clearly seen by an increase of the waveguide loss up to 7 and 6.2 dB/cm, respectively. (Inset) illustration of the cut-back method to calculate the optical loss by measuring the slope of the transmission as a function of waveguide length. (b) Comparison between the losses of the waveguide (TE-polarization) covered by photoresist cladding and the photoresist's absorption coefficient. The curves have been shifted in the vertical axis and normalized in amplitude for better comparison of the spectral features.

4. Discussion

To demonstrate the capability of Ge-rich SiGe waveguide for sensing applications, a photoresist deposited on top of the waveguide has been used to investigate the evanescent absorption of the propagating optical mode. The good correlation between photoresist's absorption spectra and waveguide loss enables to demonstrate optical sensing based on spiral waveguides of cm-lengths. While this experiment allows to retrieve the absorption signature of the photoresist between 5.2 and 6.6 µm, which already provides a sensing bandwidth larger than 400 cm^{-1}, the previously demonstrated low dispersion of the propagation characteristics of this platform up to 8.5 µm wavelength [20, 21] indicates the strong potential of this platform to sense and unambiguously identify different analytes over an even wider spectral band [26]. To further investigate the sensing capability of this waveguide in terms of

Optical Materials EXPRESS

bandwidth, the overlap factor of the optical mode with the upper cladding has also been calculated for both a waveguide spin-coated with a photoresist cladding (n~1.6) and an air-cladded waveguide. The photoresist-cladded waveguide corresponds to the reported experimental demonstration, while the air-cladded case corresponds to a gas-sensing scenario. The results reported in Fig. 5 show that the overlap factor increases with the wavelength, up to 0.61% (resp. 0.48%) in the case of photoresist-cladding (resp. air-cladding). Furthermore TE-modes overlap factors are higher than TM modes overlap factors when λ<5.6 µm while it is the opposite when λ>5.8 µm.

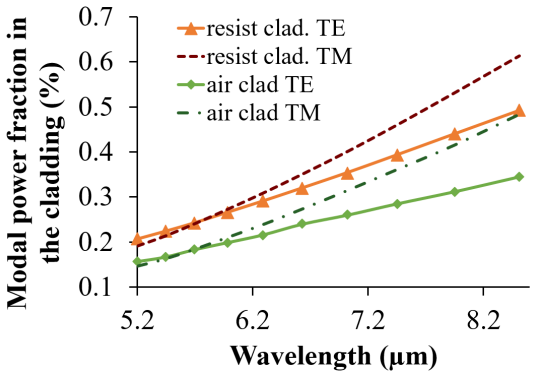

Fig. 5. Calculation of the modal power fraction in the upper cladding as a function of the operating wavelength, for both the fundamental TE and TM modes for a photoresist-cladded (n~1.6), and an air–cladded waveguide.

In order to retrieve the potential of this Ge-rich SiGe photonic integrated platform for real gas trace sensing applications, we have also estimated the minimum detectable concentration in a gas-sensing scenario. While the detection of liquid molecules is usually facilitated by their broad absorption features, gas-sensors usually require more sensitive devices to reach useful minimum detection. In the following we investigate the possibility to use the Ge-rich SiGe platform to detect the presence of methane (CH_4), which is known to play a key role in global warming [27]. CH_4 presents a strong absorption peak at 7.7 µm [6]. Waveguide loss has been previously measured around 2dB/cm at this wavelength [20]. From the simulation reported in Fig. 5 it can be seen that the overlap factor η of the optical mode in air-cladded waveguides at 7.7µm is larger than the one at 6.25 µm for photoresist-cladded waveguides. We thus decided to use the experimentally-deduced value η of 0.17% for the gas sensing evaluation, which is a conservative estimation. The optimal waveguide length L_{opt}, i.e. the length providing the optimum sensitivity for this particular case, can be deduced from the waveguide loss [3], obtaining a value of 2.17 cm. The minimum detectable concentration C_{min} is then given by the following expression [6, 3]:

$$C_{min} = \frac{-ln\left[1 - \frac{\Delta P_{min-detec}}{P_0 exp\left(-\alpha L_{opt}\right)}\right]}{\epsilon \eta L_{opt}} \quad (1)$$

where $\Delta P_{min-detec}$ is the minimum detectable variation of the optical power. This value crucially depends on the detection system and operating conditions. As an example, in the set-up used for the experiment, a DSS-MCT14 020L photodetector from Horiba was used, with a NEP of 5.10^{-12}W/Hz$^{1/2}$. By considering a signal to noise ratio of 10 and 0.1ms averaging time, $\Delta P_{min-detec}$ is 3.5 nW. Then, considering that the molar absorption of methane ϵ is 174 L mol^{-1}cm^{-1} and an optical power at the waveguide input P_0 of 1 mW, it is possible to

Optical Materials EXPRESS

estimate the lowest detectable concentration of CH_4, which is around of 1.5 x10^{-5} mol.L^{-1} (366 ppm). This value is already lower than the occupational exposure limit, of 1000 ppm, recommended by the international environmental standards [28]. Therefore, from the expected detection limit of spiral Ge-rich SiGe waveguide, such a platform has a strong potential for gas trace detection in real-time environmental applications.

Further improvements of the minimal detectable concentration are still envisioned by (i) decreasing the waveguide optical loss reducing sidewall roughness, in order to increase the optimal waveguide length and (ii) engineering the waveguide mode confinement to increase the overlap factor η of the mode with the cladding layer [20].

5. Conclusion

In summary, we demonstrated the potential of Ge-rich SiGe waveguides as a mid-IR photonic chip-scale sensor. We investigated evanescent-field absorption of the optical mode using a photoresist deposited on top of the waveguide. The absorption coefficient of the photoresist was measured separately to corroborate the results. An increase of optical mode propagation loss has been obtained at wavelengths of 5.8 and 6.2 μm, which have been clearly correlated to the absorption peaks of the photoresist. Interestingly, the sensing capability of the waveguide at larger wavelengths is only limited by the strong absorption of the photoresist from 6.6 μm and not by the inherent loss of Ge-rich SiGe waveguides, since low-loss propagation has previously been demonstrated in these waveguides up to at least a wavelength of 8.5 μm.

Finally, the sensing capability of a methane gas sensor based on the Ge-rich SiGe platform has then been discussed, showing the possibility to detect a few hundreds of ppm, which is already below the standard exposure limit. Further improvements have been proposed to boost the sensing capability up to a few tens of ppm. These results pave the way towards the demonstration of compact and portable sensors on-a-chip based on Ge-rich SiGe circuits by combining the sensing part with on-chip spectrometers and broadband nonlinear optical sources.

Funding

European Research Council (ERC) under the European Union's Horizon 2020 research and innovation program (N°639107-INsPIRE).

Acknowledgments

The fabrication of the devices was performed at the Plateforme de Micro-Nano-Technologie/C2N, which is partially funded by the "Conseil Général de l'Essonne". This work was partly supported by the French RENATECH network. The Authors also thank Michele Ortolani for his advice in setting-up the mid-IR optical measurement apparatus.